Definition and spatial location of mouse interleukin-2 residues that interact with its heterotrimeric receptor

Sandra M.Zurawski, Felix Vega,Jr, Ellen L.Doyle, Bernard Huyghe, Kevin Flaherty[1], David B.McKay[1] and Gerard Zurawski

DNAX Research Institute for Molecular and Cellular Biology, 901 California Avenue, Palo Alto, CA 94304-1104 and [1]Beckman Laboratories for Structural Biology, Department of Cell Biology, Stanford University Medical Center, Stanford, CA 94305-5400, USA

Communicated by G.Ciliberto

The high affinity receptor for interleukin-2 (IL-2) contains three subunits called IL-2Rα, β and γ. A biological and receptor binding analysis based on 1393 different mutant mouse IL-2 (mIL-2) proteins was used to define the function of each of the 149 residues. By this genetic analysis, 44 residues were assigned important functions, 21 of which were structural. The remaining 23 residues consisted of 19 residues, from three separate regions, that were important for IL-2Rα interaction; three residues, from two separate regions, that were important for IL-2Rβ interaction; and a single residue important for IL-2Rγ interaction. We built a model mIL-2 structure based on the homologous human IL-2 (hIL-2) crystal structure. The roles of the 21 residues presumed to be important for structure were consistent with the model. Despite discontinuity in the primary sequence, the residues specific for each IL-2R subunit interaction were clustered and located to three disparate regions of the tertiary mIL-2 structure. The relative spatial locations of these three surfaces are different from the two receptor binding sites known for the structurally related human growth hormone and the significance of this observation is discussed.

Key words: mutagenesis/receptor binding/structure – function

Introduction

Interleukin-2 (IL-2) is a member of a large class of protein hormones known as cytokines and lymphokines (O'Garra, 1989a,b). These hormones regulate complex immune functions via interaction with specific cell surface receptors. The functional high affinity IL-2 receptor (IL-2R, $K_D = 10^{-11}$ M) is known to contain three subunits (called α, β and γ) with single transmembrane spans. IL-2Rα is a 55 kDa protein that is a low affinity ($K_D = 10^{-8}$ M) IL-2 acceptor (Leonard et al., 1984; Nikaido et al., 1984). IL-2Rβ is a 75 kDa protein with an intracellular domain that is important for signaling (Hatakeyama et al., 1989a) and an extracellular domain that itself only weakly binds IL-2 ($K_D = 10^{-7}$ M; Ringheim et al., 1991). IL-2Rβ complexes with IL-2Rα to bind IL-2 with a fairly high affinity ($K_D = 10^{-10}$ M; Hatakeyama et al., 1989b; Ringheim et al., 1991; Imler and Zurawski, 1992). IL-2Rγ is a 64 kDa protein that itself does not bind IL-2 and complexes with IL-2Rβ to form a functional intermediate

affinity IL-2R$\beta\gamma$ ($K_D = 10^{-9}$ M; Takeshita et al., 1992) found on some lymphoid cells.

IL-2 and several other cytokines, including human growth hormone (hGH), have structures composed of a compact core bundle of four antiparallel α-helices (Bazan, 1992; McKay, 1992). IL-2Rβ and IL-2Rγ are both members of the cytokine receptor superfamily that also includes the well-studied hGH receptor (hGHR; Bazan, 1990; Cosman et al., 1990; Patthy, 1990). The hGH–hGHR interaction proceeds via a primary low affinity binding between one receptor subunit and a specific surface of the ligand. This is followed by productive binding of another identical receptor subunit to an opposite surface of the ligand (Cunningham and Wells, 1989; Cunningham et al., 1991; de Vos et al., 1992). Despite the structural commonality between IL-2 and hGH, it is unclear how accurately the hGH model can be applied to heteromeric receptors such as IL-2R. A full definition of IL-2–IL-2R interaction requires elucidation of the stoichiometry and mechanistic roles of the three receptor subunits together with localization and chemical characterization of the ligand surfaces that bind the IL-2R.

Studies of IL-2R subunits expressed in various combinations on heterologous cells have led to a good understanding of the kinetic contributions of each subunit to binding and action (Leonard et al., 1984; Nikaido et al., 1984; Hatakeyama et al., 1989b; Ringheim et al., 1991; Takeshita et al., 1992). Functional and receptor binding properties of mutant IL-2 proteins with receptor subunit-specific defects have confirmed and extended the above receptor-reconstitution data (Collins et al., 1988; Weigel et al., 1989; Zurawski and Zurawski, 1989; Zurawski et al., 1990; Sauve et al., 1991; Imler and Zurawski, 1992; Zurawski and Zurawski, 1992). The recently refined three-dimensional X-ray crystallographic structure of human IL-2 (hIL-2) permits the spatial location of these receptor subunit-specific residues (Bazan, 1992; McKay, 1992). However, only the complete definition of all IL-2R-interacting residues can provide a context for correctly modeling IL-2–IL-2R interaction.

Results and discussion

Rationale for mIL-2 substitution analysis

A complete functional map of mouse IL-2 (mIL-2) was built by systematically randomizing each codon for residues 41–142 and expressing the resulting mutant proteins in *Escherichia coli*. A previous study using deletion mutagenesis established that the 30 N-terminal and the eight C-terminal residues are dispensable for mIL-2 function (Zurawski et al., 1986; Zurawski and Zurawski, 1988). Also, we have already reported a substitution mutagenesis analysis of mIL-2 residues 31–40 (Zurawski and Zurawski, 1989). Our present study of mIL-2 residues 41–142 involved a total of 1090 different mutant proteins with an average 11 different changes per site (6–19 changes per
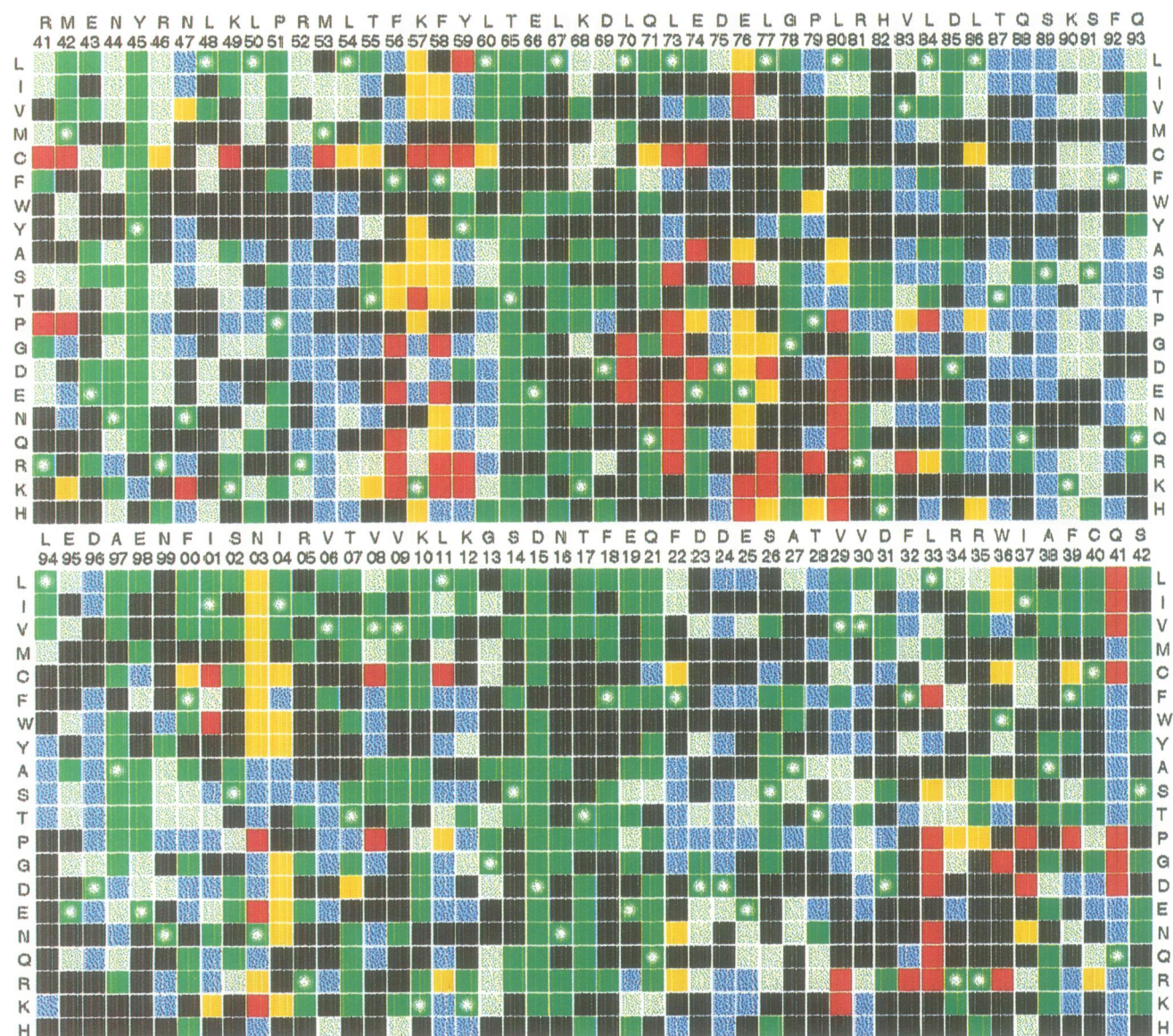
Fig. 1. Substitution analysis for mIL-2 residues 41–142. The biological properties of individual substitution proteins were defined using a bipartite HT2 cell proliferation assay which measured their biological activities in the absence and presence of the receptor antagonist mIL-2$_{Q141D}$ (Zurawski et al., 1990; Zurawski and Zurawski, 1992). Mutant proteins color-coded dark green, light green or blue had biological activities within 3-fold of mIL-2; yellow proteins had biological activities that were reduced between 5- and 25-fold; red proteins had biological activities that were reduced by >25-fold. The biological activities of dark green proteins were inhibited <10-fold by a standard concentration of mIL-2$_{Q141D}$; light green proteins were inhibited between 10- and 25-fold; and blue proteins were inhibited by >25-fold. Black squares are substitutions that were not obtained and dark green squares with white bullet marks are the wild-type residue for each position. Numbering recommences at 00 at residue 100. Note that the mIL-2$_{Q141D}$ substitution proteins have been partly described elsewhere (Zurawski et al., 1990).

site). To cope with this large data set, we first utilized a bipartite biological assay of solubilized E.coli-expressed mIL-2 proteins to identify mIL-2 residues that are important for structure or function. The rationale for this bipartite assay stems from our previous analyses of mutant mIL-2 proteins. In essence, this assay format (Zurawski et al., 1990; Zurawski and Zurawski, 1992) defines both the specific activity of the mutant protein and the degree to which that activity is antagonized by the mIL-2$_{Q141D}$ protein (Q141 substituted with D). Both of these parameters were computed relative to appropriate mIL-2 controls and together they formed the basis of the color-coded scoring scheme described in Figure 1. This scheme grades substitution mutant proteins with normal biological activities from dark green (like mIL-2), through light green and blue (normal biological activities, but subject to increasing degrees of inhibition by

mIL-2$_{Q141D}$). Mutant proteins with decreased biological activities were graded from yellow (significant decrease and generally strongly inhibited by mIL-2$_{Q141D}$) to red (very low or undetectable activity).

Identification of important residues

The color chart (Figure 1) was used to categorize the residue positions. Unimportant residues were defined as those which tolerated many different side chain replacements (dark green or light green proteins) including extreme changes of side chain type. In this category, intolerance to a few particular side chains was permitted. For example, many such residues were intolerant to Pro or Cys substitution which may cause structural disruption by, respectively, breaking α-helices or facilitating formation of inappropriate disulfides. Thus, together with data from terminal deletion analysis (Zurawski

Table I. Substitutions of mIL-2 residues 61–64

Isolate	Pro61	Lys62	Gln63	Ala64	Code[a]
43	–	Gly	Ser	–	DG
35	–	Thr	Ser	Phe	DG
39	–	Glu	Leu	Gly	DG
47	–	Val	Ile	Gly	DG
32	–	Glu	Ala	Val	DG
19	–	Pro		Val	DG
36	–	Phe	Val	Leu	DG
27	–	Phe	Met	Gly	DG
28	–	Phe	Gly	Ile	DG
14	–	Gln	Leu	Gly	LG
41	–	Pro	Ala	Thr	LG
46	–	Phe	Ile	Pro	LG
5	Gln	Arg	Lys	Leu	B
6	Lys	Thr	–	Leu	B
9	Ser	–	Gly	Gly	B
44	His	Gly	Asn	Pro	B
29	Ala	Arg	His	Ile	B
2	Gly	Ser	Gly	Ile	B
4	Lys	His	Tyr	Leu	B
21	Gly	Ser	Val	Ser	B
17	Ser	Ser	Gly	Phe	B
25	Ala	Pro	Ser	Gly	B
26	–	Pro	Gly	Gln	B

[a]Code refers to the bipartite assay criteria defined in Figure 1: DG, dark green; LG, light green; B, blue. Cassette mutagenesis was used as described (Zurawski and Zurawski, 1989) to simultaneously randomize the region encoding residues 61–64 within an mIL-2 expression plasmid. *Escherichia coli* transformants were screened to identify those that expressed full biological activity relative to mIL-2 controls. The relative resistance of these proteins to antagonism by mIL-2$_{Q141D}$ was measured as in Figure 1 and the mutated DNA sequences of the resulting plasmids were determined. Only residues that differ from native mIL-2 are shown. One isolate (#42) had the wild-type amino acid sequence.

Table II. Quantitation of binding to IL-2Rα or IL-2Rαβ

Protein	Binding	Protein	Binding
mIL-2	1[a]	V83A	280
N44S	0.7	L86R	440
N44R	140	T87R	8
R46G	12	Q88I	25
N47G	125	S89D	10
K49E	45	K90D	1
L50A	18	F92R	6
R52M	0.7	L94A	16
R52Q	110	D96A	2
M53W	60	N99K	0.6
L54K	3	N103G	2
L54G	160	K112S	3
F56V	720	D123R	4
K57D	4	D124R	30
K57E	1250	E125K	6
F58L	160	T128E	60
Y59A	380	V129T	19
Y59S	940	V130E	40
D75K	65	V130D	95
E76K	5600	D34S	2
P79S	330	D34G	2
mIL-2	1[b]	D34S	>100
Q141K	1	N99K	12
Y59A	>100	N103G	20

The upper part of the table refers to the binding to IL-2Rα of various purified mIL-2 substitution proteins. Values are fold decrease in binding relative to mIL-2 based on estimates of the amount of each protein required to competitively displace 50% of labeled hIL-2 bound to cells bearing mIL-2Rα or IL-2Rαβ (Materials and methods). The lower part refers to the binding to IL-2Rαβ determined in an analogous manner.
[a]Value is 3.2 ± 1.3×10⁻⁹ M (n = 20).
[b]Value is 2.5 ± 0.9×10⁻¹⁰ M (n = 2).

et al., 1986; Zurawski and Zurawski, 1989), 98 mIL-2 residues (or 65% of the protein) were assigned as relatively unimportant residues. Conversely, important residue positions were recognized as those intolerant to many substitutions (blue, yellow and red proteins). A subset of the important residues were hydrophobic and tolerated only conservative hydrophobic side chains or uncharged small polar side chains.

An independent combinatorial cassette mutagenesis study was used to define the side chain requirements of mIL-2 residues 61–64. This analysis (Table I) revealed a marked preference for a Pro residue at the native P61 position. Residues 62–63 tolerated many different side chains and residue 64 preferred hydrophobic and uncharged small polar side chains or no side chain.

The purpose of the initial phase of our study was to identify important residues and subsequently to select particular substitutions at these residues for the production of pure mutant proteins required for further analyses. We generally selected substitutions with the least conservative change which resulted in a protein with normal biological activity on HT2 cells but which was strongly antagonized by mIL-2$_{Q141D}$. Respectively, these properties indicated an ability of the protein to renature normally and suggested a defect in receptor interaction. In our color scheme the blue mutant proteins fit these criteria. With this strategy, circular dichroism studies (B.Huyghe *et al.*, unpublished) showed that virtually all the purified mutant proteins examined had secondary and tertiary structures that were identical or very close to those of mIL-2. Key exceptions were proteins with substitutions at a subset of the residues that preferred hydrophobic side chains. These proteins gave very low yields upon purification and were not further studied (see Materials and methods).

Assignment of receptor subunit-specific residues

We have previously characterized the biological and receptor binding properties of representative mutant mIL-2 proteins with receptor subunit-specific defects (Zurawski and Zurawski, 1989; Zurawski *et al.*, 1990; Imler and Zurawski, 1992; Zurawski and Zurawski, 1992). In particular, IL-2Rα, β and γ-defective mutant proteins have characteristic biological properties when assayed on three different IL-2-responsive mouse cell types (Zurawski and Zurawski, 1992). The first cell type, the HT2 T cell, appears to have spare IL-2R and is therefore relatively responsive to mutant mIL-2 proteins with reduced binding to IL-2R (Zurawski and Zurawski, 1992). The addition of a standard concentration of the mIL-2$_{Q141D}$ antagonist to biological assays with HT2 cells makes the assay more dependent on ligand affinity (Zurawski *et al.*, 1990; Zurawski and Zurawski, 1992) and is the basis of the bipartite assay utilized for the first part of our analysis. The second cell type, α⁺β⁺Ba/F3, are interleukin-3-responsive proB cells that are also IL-2 responsive due to transfection of mouse IL-2Rβ cDNA and auto-induction of mIL-2Rα (Zurawski and Zurawski, 1992). α⁺β⁺Ba/F3 appear to have no spare

IL-2R and mutant mIL-2 proteins with defects in IL-2Rβ and IL-2Rγ interaction elicit markedly reduced biological activities, and in some cases sub-maximal responses, on these cells (Zurawski and Zurawski, 1992). The third cell type, β^+Ba/F3, responds only to relatively high doses of mIL-2 and to mIL-2 proteins with IL-2Rα-specific defects. Mutant mIL-2 proteins with IL-2Rβ or IL-2Rγ-specific defects are inactive on this cell type (Zurawski and Zurawski, 1992).

We examined the biological responses of the above three cell lines to purified mIL-2 proteins with substitutions at important residue positions. By the above criteria, this analysis (data not shown) suggested that most of these residues were important for IL-2Rα interaction and that only two, in addition to the previously identified D34 (Zurawski and Zurawski, 1989; Zurawski *et al.*, 1990), were important for IL-2Rβ interaction. Other than the previously described Q141 (Zurawski *et al.*, 1990; Imler and Zurawski, 1992; Zurawski and Zurawski, 1992), no residues were found to be important for IL-2Rγ interaction. The inferred receptor subunit specificity of these important residue positions was confirmed by receptor binding analyses. Compared with mIL-2, the IL-2Rα-defective mutant proteins bound with various degrees of reduced affinity to fibroblastic L cells

bearing mIL-2Rα (25- to 5600-fold reduced binding compared with mIL-2, Table II). We also examined several substitution proteins at residue positions that were difficult to classify as important versus unimportant on the basis of our original criteria. These residues were often adjacent to positions that were clearly important for IL-2Rα interaction and substitutions at these residues reduced IL-2Rα binding less severely than substitutions at other clearly important positions (5- to 25-fold compared with mIL-2, Table II).

Mutant mIL-2 proteins with substitutions at N99 and N103 were specifically defective in binding associated with IL-2Rβ. These proteins bound normally to L cells bearing mIL-2Rα, but had reduced binding to L cells bearing mIL-2R$\alpha\beta$ (Table II). These binding properties are analogous to mIL-2 proteins with substitutions at the IL-2Rβ-specific residue Asp34. Proteins with substitutions at each of the three IL-2Rβ-specific residues were individually characterized by different degrees of reduction of IL-2Rβ-associated binding and of reduced biological activities (Figure 1 and Table II). We observed that certain substitutions at D34, but not N99 or N103, resulted in partial receptor-activation defects (Zurawski and Zurawski, 1992; and data not shown). These data suggest that the relative
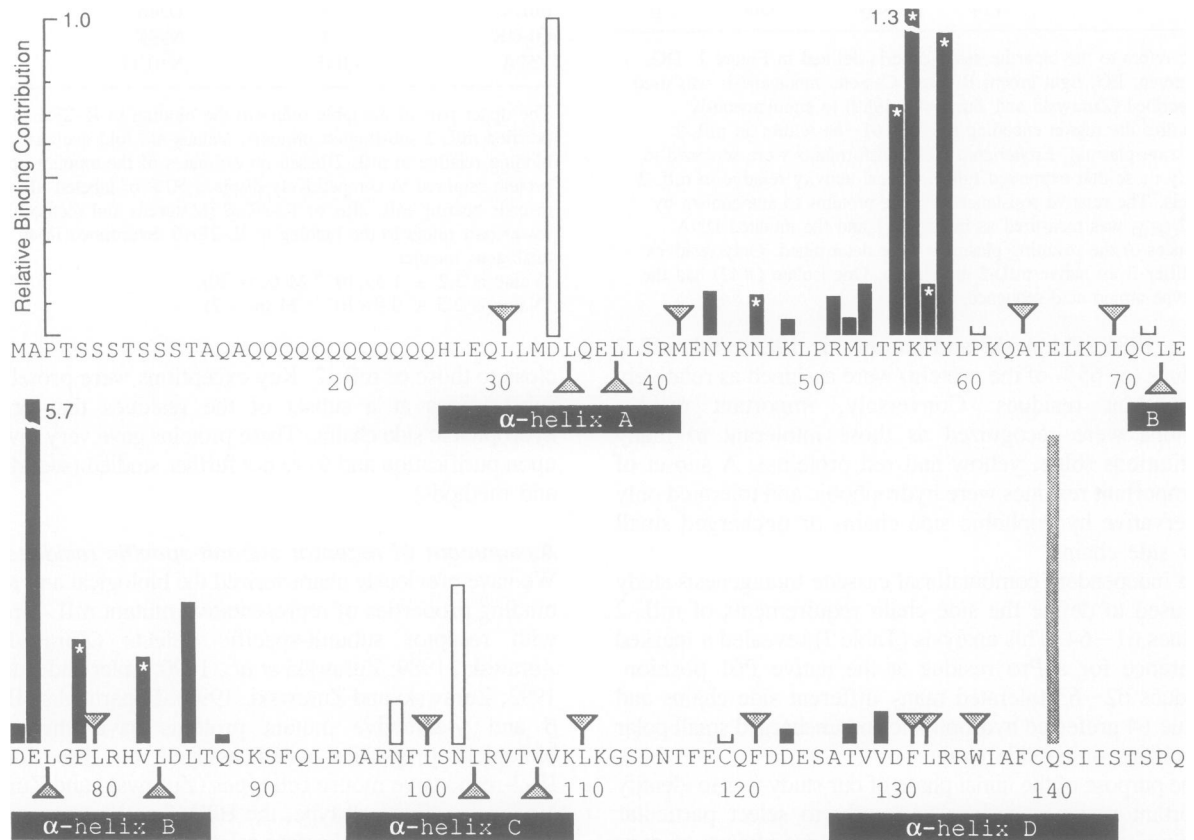

Fig. 2. Functional map of mIL-2. Bars above residues indicate positions that are important for interaction with IL-2R. The height of black bars reflects the relative contribution to IL-2Rα binding based on binding data (Table II) where a value of 1.0 reflects the existence of a substitution at this position that had 100-fold decreased binding to IL-2Rα. Asterisks indicate that the bar height is a minimal estimate since there were substitutions at these positions (Figure 1) with greater defects than those analyzed in Table II. Breaks in two of the black bars signify that they are beyond the scale by the adjacent value. The height of unfilled bars is based on an arbitrary scale that reflects the relative sensitivity (with D34 assigned an arbitrary value of 1.0) of each position to substitution as defined by the bipartite biological assay (Figure 1) and degree of reduced binding associated with IL-2Rβ (Table II). The gray bar indicates the single position important for binding associated with IL-2Rγ. Triangles indicate hydrophobic residues that are presumed to be structurally important. C72 and C120, which form a disulfide linkage, and the essential P61 are indicated by brackets. The bars under the residues define the extent of α-helical regions A–D in our model mIL-2 structure. The map is based on the properties of 1393 mutant mIL-2 proteins, 1066 of which are described in Figure 1; 24 are described in Table I. We have previously described 20 N-terminal mutant proteins (Zurawski *et al.*, 1986); 137 deletion mutant proteins (Zurawski and Zurawski, 1988); 10 D34 substitution proteins (Zurawski *et al.*, 1990); 111 residue 31–40 substitution proteins (Zurawski and Zurawski, 1989); and 25 combinatorial substitution proteins (Zurawski and Zurawski, 1989).

residue contribution to IL-2Rβ interaction is D34 > N103 > N99.

Functional map of mIL-2

The above data, together with our previously described analyses of mIL-2, now define a complete genetic map of all the functionally important residues of the 149 residue mIL-2 protein (Figure 2). This map, which is based on the described properties of 1393 mutant mIL-2 proteins, shows 23 residues which are important for interaction with IL-2R, 18 hydrophobic residues which are presumed to be part of the structural core, and three additional residues which are important for structure. These additional residues are C72−C120, which form an essential disulfide bond (Wang *et al.*, 1984; Ju *et al.*, 1987) and P61.

Spatial location of functionally important residues

The location of the various functionally important residues on the linear map raises the issue of their relative spatial locations. We addressed this by building a model mIL-2 structure for residues 30−148 based on the high resolution three-dimensional X-ray structure of hIL-2 (see Materials and methods). Over this region, hIL-2 and mIL-2 are 62% identical and 89% of the functionally important mIL-2 residues are conserved (100% if conservative changes are permitted). Also, several of these important conserved residues have been previously assigned analogous functions in hIL-2 (Wang *et al.*, 1984; Ju *et al.*, 1987; Collins *et al.*, 1988; Weir *et al.*, 1988; Sauve *et al.*, 1991).

In the model mIL-2 structure, there was a stunning correlation between residues identified as being obligatory hydrophobic structural residues and residues in the core of the molecule that have essentially zero solvent accessibility (Figure 3). The genetic analysis identified all but one (F100) of the 18 residues in the model structure with zero solvent accessibility as important residues. By the genetic analysis, 15 of these residues were assigned structural roles and three

(M53, P58, V129) were assigned roles in IL-2Rα interaction. The genetic analysis assigned only three residues with > zero solvent accessibility (A64, 7%M; L111, 9%M; F122, 23%M) as being obligatory hydrophobic structural residues (Figure 3). The apparent solvent accessibility of L111 may be artifactual, since a loop region of the molecule, which may bury the remainder of this residue, could not be built unambiguously in our model structure. F112 is unusual: in hIL-2, the aromatic ring of the tyrosine at this position packs on the disulfide, and hence its role may be unique. P61, which was identified as an obligatory residue (Table I), 'breaks' a β-strand conformation in the model structure polypeptide backbone. It is also buried and appears to contact the disulfide. Either or both of these facts may contribute to the requirement for proline at this position.

Spatial location of residues that interact with IL-2R

The 19 residues that we defined as those most important for IL-2Rα interaction form a single patch that occupies ∼1100 Å² (or ∼15% of the total) on the surface of the mIL-2 model structure (Figure 4). The residues at which substitution resulted in the greatest disruption of IL-2Rα binding are in a central position (450 Å²) within this patch. Six of the residues assigned as important for interaction with IL-2Rα (N47, M53, F58, Q76, V83, V129) had very low or zero solvent accessibility in the model structure (Figure 3) and effects on their substitution may be through disruption of the local tertiary structure necessary for binding to IL-2Rα. The remaining residues assigned as being important for interaction with IL-2Rα are significantly solvent accessible and are most likely to interface directly with IL-2Rα (Figure 3).

The three residues (D34, N99, N103) that we defined as most important for IL-2Rβ interaction form a single patch on a face away from the IL-2Rα binding surface (∼18 Å; Figure 4). We noted a particularly interesting feature regarding the major IL-2Rα- and IL-2Rβ-interacting residues
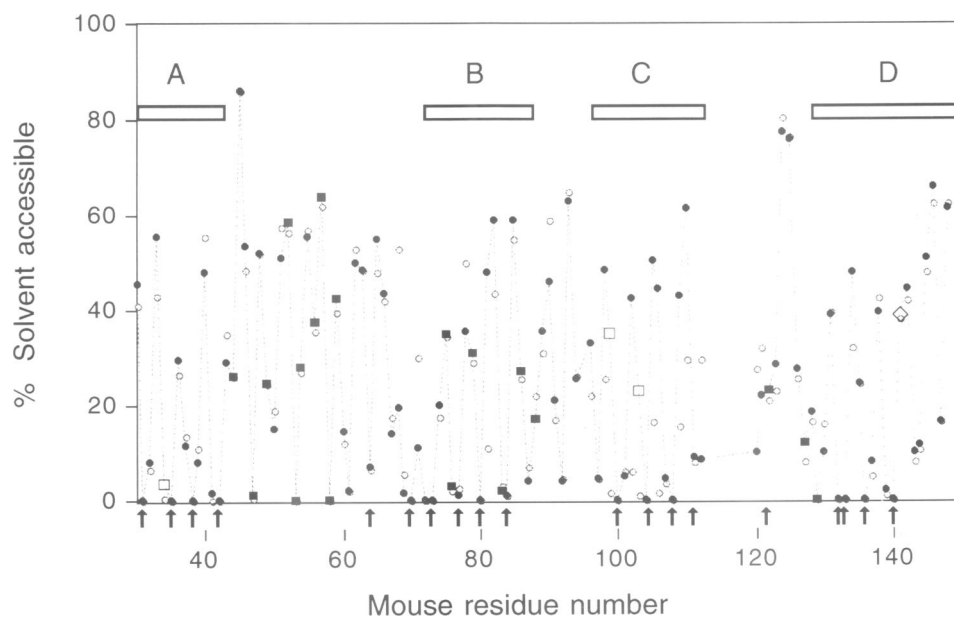

Fig. 3. Plot of percentage that is solvent accessible for the surface of each residues (Materials and methods). Numbering is for the mIL-2 sequence. mIL-2 residues: filled squares, IL-2Rα-interacting; open squares, IL-2Rβ-interacting; open diamond, IL-2Rγ-interacting; filled circles, remaining. Open circles are one promoter of hIL-2. Bars delimit α-helical residues of the four-helix core of the molecule. Arrows below abscissa show mIL-2 residues identified as obligatory hydrophobic.
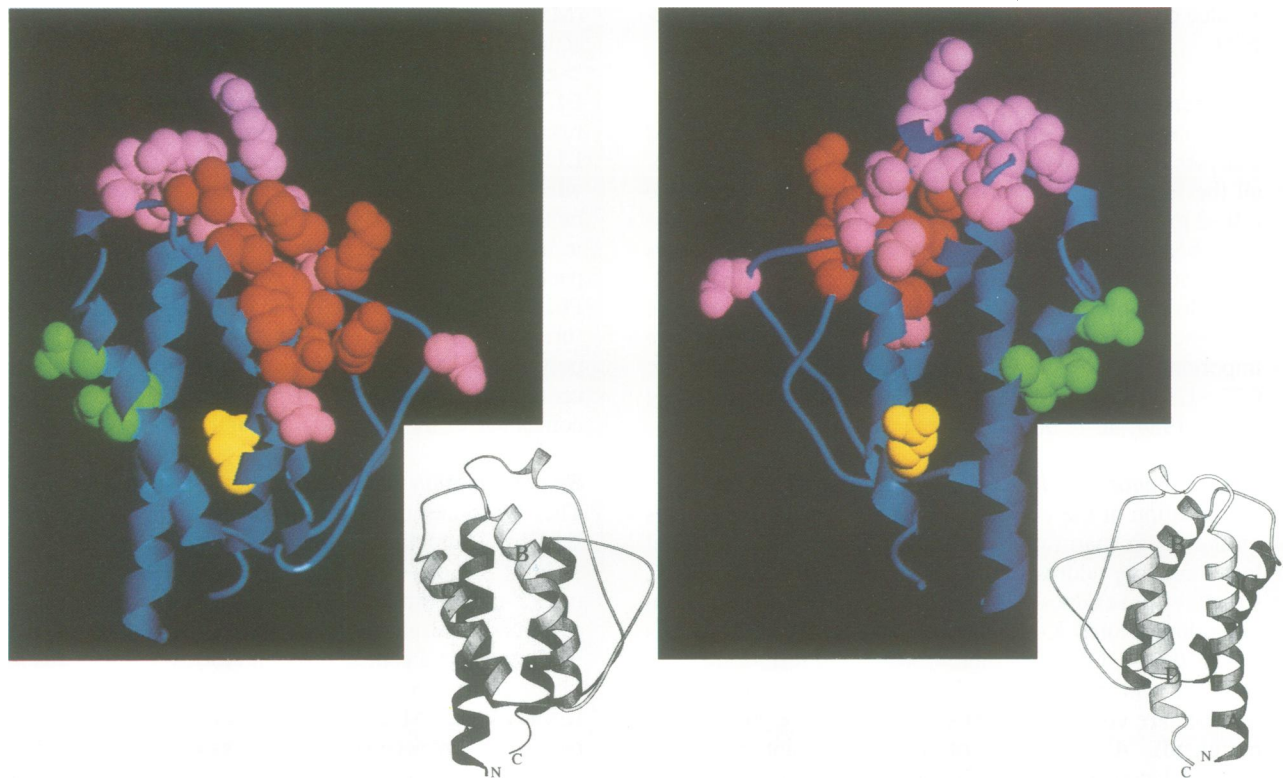
Fig. 4. Structural model of mIL-2 showing important IL-2R-interacting residues. The two representations, which are rotated 180° relative to each other, were constructed using the program RIBBON (Carson and Bugg, 1986). The side chains and Cα atoms of the important IL-2R-interacting residues are shown space filled. The colors are: red, strong IL-2Rα-interacting; pink, weaker IL-2Rα-interacting; green, IL-2Rβ-interacting; yellow, IL-2Rγ-interacting. The accompanying uncolored schematics indicate the positions of the four α-helices.

(Q76, D34). Both these acidic residues are <2% solvent-exposed in the hIL-2 structure, although in both cases the carboxyl groups are at the surface of the protein in crevices. None of the other acidic or basic residues in the molecule are so solvent inaccessible. This may be evidence of structural 'shielding' of a charged residue that is critical for binding in order to reduce competition from non-specific electrostatic interactions with other proteins or ions.

Lastly, the single IL-2Rγ-interacting residue (Q141) is on a surface that is relatively distant from the IL-2Rα- and IL-2Rβ-interacting regions (~21 Å and ~18 Å, respectively; Figure 4).

Conclusion: IL-2R as a model for the cytokine receptor superfamily

The hGH/hGHR system has been very well studied by mutational, biochemical and structural analyses (Cunningham and Wells, 1989; Cunningham *et al.*, 1991; de Vos *et al.*, 1992). The ligand and two of the receptor components (β and γ) of the IL-2/IL-2R system have structural homologs in the hGH/hGHR system (Bazan, 1992; de Vos *et al.*, 1992; Takeshita *et al.*, 1992) and it is pertinent to compare the dispositions and natures of the binding sites on the two ligands. The primary binding event for hGH is the interaction of one ligand surface (called site I) with one hGHR chain. Site I is a 1230 Å² patch of both hydrophilic and hydrophobic residues from the N-terminal part of α-helix A, the distal part of the α-helix A−B loop and the C-terminal half of α-helix D (de Vos *et al.*, 1992). An opposite face of hGH (called site II) binds a second hGHR chain, and this ligand-induced dimerization is thought to invoke signal transduction (de Vos *et al.*, 1992). It is difficult to see a close

parallel of these events in the IL-2/IL-2R system. Alone, the IL-2 subunits have an IL-2 binding hierarchy of $\alpha > \beta > \gamma$ (see Introduction). For high affinity IL-2R, the primary binding subunit is IL-2Rα which binds IL-2 with a characteristic rapid on-rate (Ringheim *et al.*, 1991). The preponderance of important residues that are specific for IL-2Rα interaction is consistent with a primary binding role for this subunit. Our minimal estimate, which does not take into account several additional residues that make relatively minor binding contributions, of the mIL-2 surface area specific for IL-2Rα interaction is 1100 Å². This surface is comparable in extent and contribution by both hydrophilic and hydrophobic residues to the primary (site I) binding face of hGH (de Vos *et al.*, 1992). However, the IL-2Rα-interacting site is composed of residues from the proximal part of the α-helix A−B loop, α-helix B and the N-terminal tip of α-helix D and this disposition is markedly different from hGH site I.

Although it is 100-fold weaker than that to cells with high affinity IL-2R, IL-2-binding to cells which lack IL-2Rα can elicit productive signaling (see Introduction). Such 'intermediate affinity' IL-2R are composed of IL-2Rβ and γ (Hatakeyama *et al.*, 1989b). Unlike IL-2Rα, IL-2Rβ and γ are members of the hematopoietic receptor superfamily and their interaction with IL-2 may be more analogous to the binding of hGH to hGHR. Indeed, there is concordance between the dispositions of hGH site II and the IL-2Rβ-interacting site, which are both formed from residues in α-helices A and C (de Vos *et al.*, 1992). There is also evidence that at least one of the IL-2Rβ-interacting residues (D34) directly contacts IL-2Rβ (Imler *et al.*, 1992) and that association of IL-2Rγ with IL-2R is IL-2 dependent

(Takeshita *et al.*, 1992). If the interaction of IL-2Rβγ with IL-2 were indeed analogous to the hGH – hGHR interaction, then it is relevant that not all of the hGH surface interfaces the two hGHR subunits (de Vos *et al.*, 1992). It is possible that IL-2α interaction evolved to stabilize a relatively weak IL-2 – IL-2Rβγ complex by utilizing interactions with the exposed IL-2 surface in this complex. This notion is supported by our observations that all three IL-2R-interacting regions are relatively distant from one another.

Our chemical definition and spatial location of three separate IL-2R-interacting surfaces of IL-2 should facilitate rational design of small chemical analogs of IL-2 action. However, further studies will be required, including elucidation of the stoichiometry of the ligand and subunits within productive IL-2 – IL-2R complexes and definition of possible conformational changes associated with IL-2 binding, before a complete mechanistic picture emerges of IL-2 action upon IL-2R.

Materials and methods

Substitution analysis of mIL-2
Methods have been previously described for expression of mIL-2 and mutant mIL-2 proteins in *E.coli* (Zurawski *et al.*, 1986; Zurawski and Zurawski, 1988), cassette substitution mutagenesis (Zurawski and Zurawski, 1989), and preparation and biological assay of crude extracts of mutant mIL-2 proteins in the presence and absence of the mIL-2$_{Q141D}$ antagonist protein (Zurawski and Zurawski, 1988; Zurawski *et al.*, 1992).

Receptor binding analysis
Receptor binding analyses were performed on L cells expressing mIL-2Rα (A22 cell line) as described (Zurawski and Zurawski, 1992) and utilized a heterologous displacement format with the labeled ligand ([^{125}I]hIL-2, IM 247 Amersham; or [^{32}P]mIL-2.P2; Imler and Zurawski, 1992) at 10^{-9} M and various concentrations of purified mIL-2 or mutant mIL-2 proteins. mIL-2 proteins were purified as described (Zurawski and Zurawski, 1992; B.Huyghe *et al.*, unpublished). Data for mIL-2 and some representative mutant mIL-2 proteins were analyzed using the Ligand computer program (Munson and Rodbard, 1980). This analysis established that the IL-2Rα of A22 cells bound mIL-2 with a dissociation constant of $K_D = 3 \times 10^{-9}$ M and that the estimated decreases in IL-2Rα binding of mutant mIL-2 proteins shown in Table II were directly proportional to increases in their dissociation constants. The standard error divided by the value of dissociation constant estimates was <16%. Receptor binding analyses were also performed on L cells expressing mIL-2Rαβ (this cell line was derived by co-transfection by expression plasmids for mIL-2Rα and mIL-2Rβ) as described above except that the labeled ligand was at 10^{-11} M.

mIL-2 model structure
The amino acid sequence of mIL-2 from residue 31 through the penultimate P148 can be aligned with the amino acid sequence of hIL-2 with 62% identity and a single amino acid insert at position Q95 of mIL-2 relative to hIL-2 (Bazan, 1992). A model for the mIL-2 protein was generated from the hIL-2 structure (McKay, 1992) by replacing the amino acid residues of the human molecule with those of the mouse, and manually adjusting the conformations of side chains to remove severe steric clashes. Residue Q95 of IL-2 (an unimportant residue, Figure 1) was deleted. Although the mIL-2 model is presumably incorrect in some details of side chain conformation, it is assumably accurate enough to reveal the general spatial location of amino acid residues.

Solvent-exposed surface areas for residues were computed with the program package XPLOR (Brunger *et al.*, 1985), which uses the algorithm of Lee and Richards (1971). To compute the fraction of surface area that is solvent exposed the total surface area was computed for the residue in vacuum as the middle residue in a tripeptide G-X-G, where the conformation of the tripeptide was identical to that found in the hIL-2 structure. Solvent-accessible surface areas were computed for both protomers in the crystallographic asymmetric unit of hIL-2 crystals, as well as for the mIL-2 model.

Assignment of hydrophobic residues
Eighteen residues were designated as preferring hydrophobic side chains and as probably important for maintaining mIL-2 structure: L31, L35, L38,

M42, A64, L70, L73, L77, L80, L84, I101, I104, V108, L111, F122, F132, L133, W136. The basis for these assignments for positions 31, 35 and 38 was previous data (Zurawski and Zurawski, 1989); for position 64, the side chain preferences shown in Table I; for positions 42, 70, 80, 133 and 136, side chain preferences shown in Figure 1; for positions 73, 77, 84, 101, 104, 108, 111, 122 and 132, side chain preferences shown in Figure 1 together with very poor yields of proteins with particular substitutions at these positions. Poor yields (< 100 μg per 12 l of shake flask culture) were observed for the following proteins prepared by our standard method (which generally yielded >1 mg per batch, B.Huyghe *et al.*, unpublished): L54N, F58H, F58D, F58N, L73A, L77Y, L84H, I101D, I104Y, V108N, L111E, K112E, K112S, F122H, F132I.

References

Bazan,J.F. (1990) *Proc. Natl Acad. Sci. USA*, **87**, 6934–6938.
Bazan,J.F. (1992) *Science*, **257**, 410–413.
Brunger,A.T., Kuriyan,J. and Karplus,M. (1985) *Science*, **235**, 458–460.
Carson,M. and Bugg,C.E. (1986) *J. Mol. Graph.*, **4**, 121–122.
Collins,L., Tsien,W.H., Seals,C., Hakimi,J., Weber,D., Bailon,P., Hoskins,J., Greene,W.C., Toome,V. and Ju,G. (1988) *Proc. Natl Acad. Sci. USA*, **85**, 7709–7713.
Cosman,D., Lyman,S.D., Idzerda,R.L., Beckmann,M.P., Park,L.S., Goodwin,R.G. and March,C.J. (1990) *Trends Biochem. Sci.*, **15**, 265–270.
Cunningham,B.C. and Wells,J.A. (1989) *Science*, **244**, 1081–1085.
Cunningham,B.C., Ultsch,M., De,V.A., Mulkerrin,M.G., Clauser,K.R. and Wells,J.A. (1991) *Science*, **254**, 821–825.
de Vos,A.M., Ultsch,M. and Kossiakoff,A.A. (1992) *Science*, **255**, 306–312.
Hatakeyama,M., Mori,H., Doi,T. and Taniguchi,T. (1989a) *Cell*, **59**, 837–845.
Hatakeyama,M., Tsudo,M., Minamoto,S., Kono,T., Doi,T., Miyata,T., Miyasaka,M. and Taniguchi,T. (1989b) *Science*, **244**, 551–556.
Imler,J.-L. and Zurawski,G. (1992) *J. Biol. Chem.*, **267**, 13185–13190.
Imler,J.-L., Miyajima,A. and Zurawski,G. (1992) *EMBO J.*, **11**, 2047–2053.
Ju,G., Collins,L., Kaffka,K.L., Tsien,W.H., Chizzonite,R., Crowl,R., Bhatt,R. and Kilian,P.L. (1987) *J. Biol. Chem.*, **262**, 5723–5731.
Lee,B. and Richards,F.M. (1971) *J. Mol. Biol.*, **55**, 379–400.
Leonard,W.J., Depper,J.M., Crabtree,G.R., Rudikoff,S., Pumphrey,J., Robb,R.J., Kronke,M., Svetlik,P.B., Peffer,N.J. and Waldmann,T.A. (1984) *Nature*, **311**, 626–631.
McKay,D.B. (1992) *Science*, **257**, 412–413.
Munson,P.J. and Rodbard,D. (1980) *Anal. Biochem.*, **107**, 220–239.
Nikaido,T., Shimizu,A., Ishida,N., Sabe,H., Teshigawara,K., Maeda,M., Uchiyama,T., Yodoi,J. and Honjo,T. (1984) *Nature*, **311**, 631–635.
O'Garra,A. (1989a) *Lancet*, i, 943–947.
O'Garra,A. (1989b) *Lancet*, i, 1003–1005.
Patthy,L. (1990) *Cell*, **61**, 13–14.
Ringheim,G.E., Freimark,B.D. and Robb,R.J. (1991) *Lymphokine Cytokine Res.*, **10**, 219–224.
Sauve,K., Nachman,M., Spence,C., Bailon,P., Campbell,E., Tsien,W.H., Kondas,J.A., Hakimi,J. and Ju,G. (1991) *Proc. Natl Acad. Sci. USA*, **88**, 4636–4640.
Takeshita,T., Asao,H., Ohtani,K., Ishii,N., Kumaki,S., Tanaka,N., Munakata,H., Nakamura,M. and Sugamura,K. (1992) *Science*, **257**, 379–382.
Wang,A., Lu,S.-D. and Mark,D.F. (1984) *Science*, **224**, 1431–1433.
Weigel,U., Meyer,M. and Sebald,W. (1989) *Eur. J. Biochem.*, **180**, 295–300.
Weir,M.P., Chaplin,M.A., Wallace,D.M., Dykes,C.W. and Hobden,A.N. (1988) *Biochemistry*, **27**, 6883–6892.
Zurawski,S.M. and Zurawski,G. (1988) *EMBO J.*, **7**, 1061–1069.
Zurawski,S.M. and Zurawski,G. (1989) *EMBO J.*, **8**, 2583–2590.
Zurawski,S.M. and Zurawski,G. (1992) *EMBO J.*, **11**, 3905–3910.
Zurawski,S.M., Mosmann,T.R., Benedik,M. and Zurawski,G. (1986) *J. Immunol.*, **137**, 3354–3360.
Zurawski,S.M., Imler,J. and Zurawski,G. (1990) *EMBO J.*, **9**, 3899–3905.

Received on July 29, 1993